pISSN 1229-845X, eISSN 1976-555X
J. Vet. Sci. (2014), **15**(3), 455-458
http://dx.doi.org/10.4142/jvs.2014.15.3.455
Received: 14 Oct. 2013, Revised: 31 Dec. 2013, Accepted: 22 Feb. 2014

JOURNAL OF
Veterinary
Science

Case Report

Clinical applications and characteristics of apparent diffusion coefficient maps for the brain of two dogs

Boeun Kim, Kangjae Yi, Sunyoung Jung, Seoyeon Ji, Mincheol Choi, Junghee Yoon*

College of Veterinary Medicine and the Research Institute for Veterinary Science at Seoul National University, Seoul 151-742, Korea

Diffusion-weighted imaging (DWI) and apparent diffusion coefficient (ADC) mapping are functional magnetic resonance imaging techniques for detecting water diffusion. DWI and the ADC map were performed for intracranial lesions in two dogs. In necrotizing leukoencephalitis, cavitated lesions contained a hypointense center with a hyperintense periphery on DWI, and hyperintense signals on the ADC maps. In metastatic sarcoma, masses including a necrotic region were hypointense with DWI, and hyperintense on the ADC map with hyperintense perilesional edema on DWI and ADC map. Since DWI and ADC data reflect the altered water diffusion, they can provide additional information at the molecular level.

Keywords: apparent diffusion coefficient map, brain, diffusion-weighted imaging, dog, magnetic resonance image

Diffusion-weighted imaging (DWI) and apparent diffusion coefficient (ADC) mapping are functional magnetic resonance (MR) imaging techniques used to detect the random movement of water molecules (diffusion) affected by various brain lesions. DWI is performed by applying diffusion gradients to a T2-weighted (T2W) spin-echo sequence. Because hyperintense signal acquired with DWI is related to a long T2 relaxation time (known as the T2 shine through effect) as well as reduced water diffusion, ADC values are calculated based on DWI data obtained with at least two different b-values to eliminate the T2 shine through effect. These values represent a quantitative expression of water diffusion within the voxel and are displayed on an ADC map.

Unrestricted water diffusion, such as cerebrospinal fluid (CSF), produces low signal intensity on DWI and a high ADC. Conversely, restricted diffusion of water with a low ADC produces high signal intensity on DWI [6,11]. DWI and the ADC have been routinely used in human medicine to diagnose stroke. Additionally, numerous studies of non-infarct lesions have been published including ones on tumor grading for prognosis determination, biopsy target selection, treatment monitoring, differentiation between epidermoid tumors and arachnoid cysts, and imaging features of infection and variable encephalopathy [1,2,5-7,9-12,14]. In veterinary medicine, there are several reports of clinical MR image findings associated with infarct based on DWI and ADC results in dogs [3,8]. Additionally, an investigation about the clinical use of DWI and ADC to evaluate non-infarct lesions such as tumors and ones related to inflammatory disease was recently published [13]. The goal of the current study was to describe MR imaging findings including ones generated by DWI and ADC map for two dogs with intracranial lesions. These findings were compared with results of a histopathologic examination. Furthermore, the clinical relevance of diffusion imaging with a low field magnet was evaluated.

A 9-month-old, neutered female Maltese (Case 1) was referred to the Seoul National University Veterinary Medical Teaching Hospital (SNU VMTH; Korea) with a 2-day history of left head turning. During the physical examination, the patient was depressed and presented ataxia, head turning, circling to the left side, and ventrolateral strabismus. A proprioceptive deficit on the right forelimb and bilateral hindlimb was observed although the patient was somewhat uncooperative. Blood test findings revealed mildly elevated creatinine kinase, calcium, and phosphorus levels. Canine distemper kit results were negative. No remarkable thorax, abdomen, cervical vertebra, skull, or abdominal ultrasonography findings were observed.

MR imaging of the brain was performed using a 0.3 Tesla (T) open permanent magnet (AIRIS Vento; Hitachi, Japan). Multiple sequences including T1-weighted (T1W),

*Corresponding author: Tel: +82-2-880-1265; Fax: +82-2-880-1211; E-mail: heeyoon@snu.ac.kr

T2W, fluid-attenuated inversion recovery (FLAIR), gradient echo (GE), and contrast-enhanced T1W images (0.1 mmol/kg, Dotarem; Guerbet, France) were obtained in the sagittal, dorsal, and transverse planes with a slice thickness of 2.5 to 2.8 mm. In addition, DWI was performed using b-factors of 0 and 800 seconds/mm^2 with a slice thickness of 5.5 mm. ADC values were calculated based on the DWI data and ADC maps were automatically generated by MR central processing unit (AIRIS Vento; Hitachi).

MR imaging (Fig. 1) revealed the presence of multiple, extensive, and irregularly shaped lesions in the cerebrum and left brainstem. The lesions were mainly found in the subcortex and white matter, and were isointense to hypointense on the T1W images and hyperintense on the T2W and FLAIR images. Cavitated lesions in the right temporal lobe, left occipital lobe, and caudal region of the left temporal lobe had markedly hyperintense signals on the T2W images. Additionally, these lesions contained a hypointense center with a hyperintense periphery on the FLAIR images. On the diffusion images recovered with DWI, the cavitated lesion had a hypointense center with a hyperintense periphery. Hyperintense signals were observed on the ADC maps.

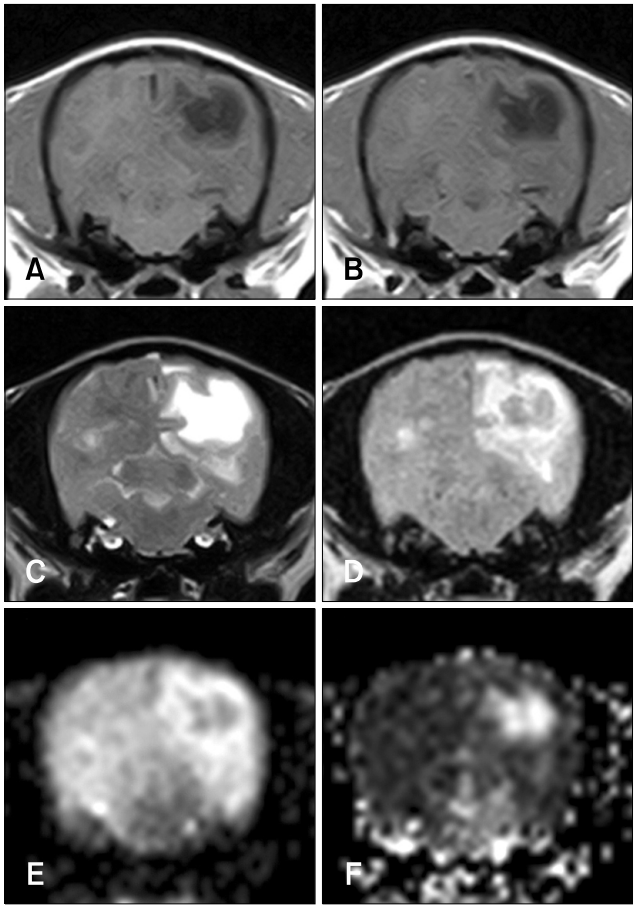

Fig. 1. Transverse magnetic resonance (MR) images of Case 1. There was a marked cavitary lesion in the left occipital lobe. This cavitated lesion appeared hypointense on the T1-weighted (T1W) image (A) without contrast enhancement (B). The T2-weighted (T2W) image (C) had marked hyperintensity in this region. On the fluid-attenuated inversion recovery image (D), the lesion contained a hypointense center with a hyperintense periphery. On the diffusion images, the cavitated lesion contained a hypointense center with a hyperintense periphery on the diffusion-weighted imaging (DWI) (E) and a hyperintense signal on the apparent diffusion coefficient (ADC) maps (F).

A CSF sample was obtained by puncturing the cisterna magna. CSF evaluation was non-diagnostic due to the presence of abundant erythrocytes [the total nucleated cell count was 134 cells/μL, and protein content was 500 mg/dL according to the dipstick (Combur^{10}Test; Roche diagnostic, Switzerland)]. Analysis of the CSF with a canine distemper kit produced negative results. Clinical symptoms worsened for two days and the dog was euthanized at the owner's request. A histopathologic survey of the brain was subsequently performed. Gross examination revealed hyperemia and edematous change in the brain. Multiple greyish discolorations were observed mostly in the white matter. Cavitations were identified in the right temporal lobe and caudal to the left temporal lobe. There was a small hemorrhagic area in the left brainstem. Histologically, there were multiple inflammatory nodules primarily in the white matter with perivascular cuffing along with infiltration of gitter cells, lymphocytes, and plasma cells. In the cavitary area, histologic cavitation and infiltration of gitter cells and gemistocytes were found. There was no evidence of infection. Severe cerebral encephalomalacia and gliosis were considered, and the dog was ultimately diagnosed with necrotizing leukoencephalitis (NLE).

A 10-year-old, intact female cocker spaniel (Case 2) was referred to the SNU VMTH for oronasal fistula repair. Blood test results revealed the presence of mild anemia, leukocytosis, increased levels of sodium, phosphorous, and creatinine kinase; and decreased potassium concentrations. Hyposthenuric urine and proteinuria were identified by urinalysis. A lung mass was found by thoracic radiography performed in the referring hospital, but the owner declined additional examination. Tooth extraction and alveolar bone sequestrum repair were performed under general anesthesia. After recovering from anesthesia, the patient displayed right head turning, circling, and seizures.

Brain MRI was performed the next day using a 0.3 T open permanent magnet (AIRIS Vento; Hitachi). Multiple sequences including T1W, T2W, FLAIR, GE, and contrast-enhanced T1W images (0.1 mmol/kg, Dotarem; Guerbet) were obtained in the sagittal, dorsal, and transverse planes with a slice thickness of 2.0 to 2.6 mm. In addition, DWI was performed using a b-factor of 0 and 800 sec/mm^2 with a slice thickness of 2.0 to 2.6 mm. ADC values were calculated based on the DWI results and ADC

maps were generated by automated software.

With MR imaging (Fig. 2), multiple well-demarcated round masses in the forebrain and cerebellum were observed. The lesions had isointense signals on T1W and FLAIR images without contrast enhancement and isointense to hypointense signals were found on the T2W images. A midline shift was identified indicating a mass effect. Round masses had a low DWI signal and high signal on the ADC maps. Perilesional areas were isointense on the T1W images and hyperintense on the T2W images. Perilesional edema had a high signal on DWI and ADC maps. Thoracic computed tomography (CT) was also performed and a contrast-enhanced round mass was identified in the accessary lung lobe. There were multiple small nodules in the lung lobe as well as enlarged sternal and tracheobronchial lymph nodes with contrast enhancement.

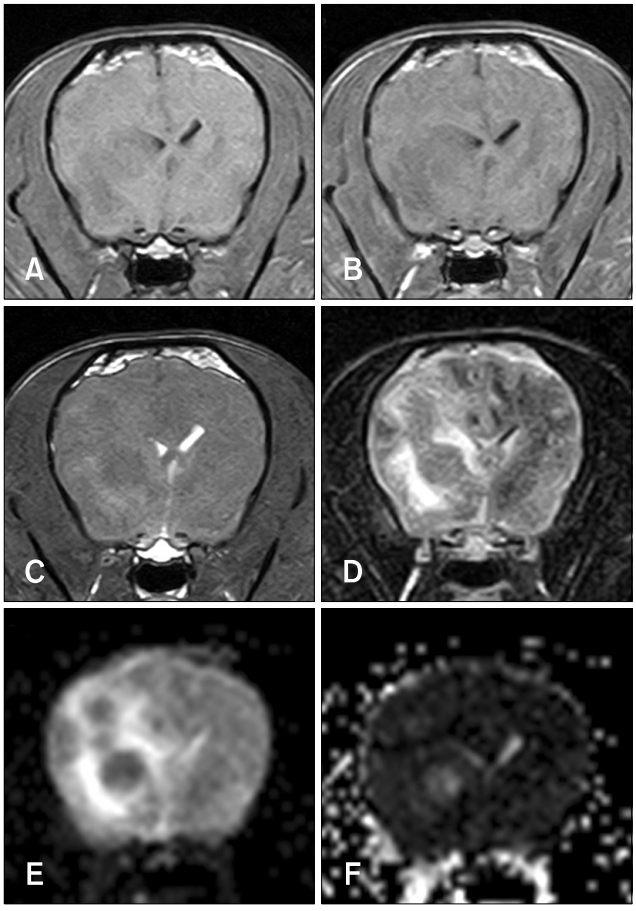

Fig. 2. Transverse MR images of Case 2. There were multiple round masses in the forebrain with a mass effect. The masses contained an isointense signal on the T1W image (A) without contrast enhancement (B) along with isointense to hypointense signals on the T2W images (C). These lesions had a low signal on DWI analysis (E) and a high signal on the ADC map (F). Perilesional edema generated a hyperintense signal with DWI (E) and on the ADC map (F).

After MRI and CT were performed, the patient did not regain consciousness and artificial respiration was stopped at the owner's request. CSF analysis was not conducted but a histopathologic examination was performed. Neoplastic proliferation originating from mesenchymal cells was identified in the hard palate. Multiple nodules containing the same cells were found in the lung, heart, kidney, and adrenal gland. In the brain, clearly demarcated round nodules in the right frontal to the temporal lobe and thalamus were found. Brain lesions contained mesenchymal cells and necrotic regions of varying size. Microscopically, multiple areas of infiltration by abundant neutrophils and a small number of lymphocytes were identified in the lesions. The dog was diagnosed with metastatic sarcoma having necrotic regions in the brain.

NLE confirmed by histopathologic examination in Case 1 was associated with a high signal on DWI and ADC maps as well as cavitary regions. The imaging results were consistent with necropsy findings. To the best of our knowledge, this is the first trial to use DWI and ADC for identifying dogs with NLE although there is a single report on the application of diffusion imaging in a canine with inflammatory disease [13]. Inflammatory lesions including ones associated with granulomatous meningoencephalitis (GME), lymphocytic perivascular inflammation, histiocytic inflammation, and radiation-induced leukoencephalitis have various features. In particular, GME, a common non-infectious inflammatory disease, has low ADC values characterized by restricted water diffusion unlike our case [13]. In humans with herpes encephalitis, most lesions are accompanied by cytotoxic edema and have low ADC values. High ADC values associated with vasogenic edema are rarely identified [5,12,14]. Additionally, it has been reported that cytotoxic edema indicates fulminant necrotizing changes while vasogenic edema is linked to early infectious inflammatory disease with edema. Encephalitis accompanied by vasogenic edema has a good prognosis if prompt therapy is administered [12]. Diffusion images for humans with non-infectious inflammatory disease such as GME, NLE, or necrotizing meningoencephalitis have not been and a limited number of cases have been reported in the veterinary medicine literature. Diffusion enables clinicians to better detect early inflammation compared to conventional MR sequences, and provides information on disease severity and response to treatment [14].

In Case 2, the lesions were not clearly identified on T1W, T2W, or contrast-enhanced T1W images although multiple masses were found on the FLAIR and diffusion images due to perilesional edema. Given the circumstances mentioned above, a diagnosis of a metastatic tumor with a lung mass and nodules was considered. It is difficult to visually differentiate brain abscess from cystic or necrotic brain tumors based on conventional MR images [1,10]. All brain abscesses have low ADC values indicative of restricted

diffusion due to pus in the abscess cavity [1,2]. Most cystic or necrotic tumors such as malignant glioma or metastases have high ADC values compared to normal brain [1,9,10]. Intra-cavity fluid that is less viscous than fluid found in abscesses is responsible for high ADC values [7,10]. One exceptional case of a tumor had diffusion characteristics similar to those of an abscess due to early stage necrosis without liquefaction [4]. Hyperintense signals on the ADC maps can rule out an abscess while necrotic or cystic portions of a brain tumor may possibly be identified with diffusion images.

Lesions in Case 2 had actual necrotic regions observed during histopathologic examination. Additionally, there was perilesional edema around the multiple round masses associated with isointense signals on the T1W as well as high signals on T2W and FLAIR images. Perilesional edema produced high signal intensity with DWI and on the ADC map. Vasogenic edema was usually associated with elevated vascular permeability and increased extracellular fluid in white matter tumors, which was consistent with perilesional edema of Case 2 exhibiting elevated ADC [11,15]. Tumor malignancy corresponds to high cellularity and low ADC values. Thus, tumor grading based on diffusion characteristics can be accomplished with non-invasive methods. The formulation of treatment plans and prognosis evaluation would therefore be completed without invasive biopsy [5-7,11].

The cases in this report demonstrated the feasibility of diffusion MR imaging and potential clinical application for analyzing non-infarct lesions. Despite the limited number of cases, diffusion images were obtained with 0.3 T low-field MR. Images associated with non-infectious inflammatory disease were obtained unlike previous reports in the veterinary literature. Additionally, cystic or necrotic tumor characteristics identified on the ADC maps were consistent with those reported in previous studies. DWI and ADC have been valuable tools for diagnosing ischemic infarction and evaluating non-infarct lesions based on signal intensity on the ADC map. These methods provide additional information about lesions at the molecular level. It can help characterize lesions more specifically and accurately. By studying more cases confirmed by histopathologic examination, the accuracy of diagnoses based on MR imaging will be further improved. This will help clinicians plan therapies, evaluate disease prognosis based on tumor grading along with inflammation severity, and monitor responses to treatment.

Conflict of Interest

There is no conflict of interest.

References

1. **Chang SC, Lai PH, Chen WL, Weng HH, Ho JT, Wang JS, Chang CY, Pan HB, Yang CF.** Diffusion-weighted MRI features of brain abscess and cystic or necrotic brain tumors: comparison with conventional MRI. Clin Imaging 2002, **26**, 227-236.
2. **Desprechins B, Stadnik T, Koerts G, Shabana W, Breucq C, Osteaux M.** Use of diffusion-weighted MR imaging in differential diagnosis between intracerebral necrotic tumors and cerebral abscesses. AJNR Am J Neuroradiol 1999, **20**, 1252-1257.
3. **Garosi L, McConnell JF, Platt SR, Barone G, Baron JC, de Lahunta A, Schatzberg SJ.** Clinical and topographic magnetic resonance characteristics of suspected brain infarction in 40 dogs. J Vet Intern Med 2006, **20**, 311-321.
4. **Holtås S, Geijer B, Strömblad LG, Maly-Sundgren P, Burtscher IM.** A ring-enhancing metastasis with central high signal on diffusion-weighted imaging and low apparent diffusion coefficients. Neuroradiology 2000, **42**, 824-827.
5. **Karaarslan E, Arslan A.** Diffusion weighted MR imaging in non-infarct lesions of the brain. Eur J Radiol 2008, **65**, 402-416.
6. **Koh DM, Collins DJ.** Diffusion-weighted MRI in the body: applications and challenges in oncology. AJR Am J Roentgenol 2007, **188**, 1622-1635.
7. **Krabbe K, Gideon P, Wagn P, Hansen U, Thomsen C, Madsen F.** MR diffusion imaging of human intracranial tumours. Neuroradiology 1997, **39**, 483-489.
8. **McConnell JF, Garosi L, Platt SR.** Magnetic resonance imaging findings of presumed cerebellar cerebrovascular accident in twelve dogs. Vet Radiol Ultrasound 2005, **46**, 1-10.
9. **Nadal Desbarats L, Herlidou S, de Marco G, Gondry-Jouet C, Le Gars D, Deramond H, Idy-Peretti I.** Differential MRI diagnosis between brain abscesses and necrotic or cystic brain tumors using the apparent diffusion coefficient and normalized diffusion-weighted images. Magn Reson Imaging 2003, **21**, 645-650.
10. **Park SH, Chang KH, Song IC, Kim YJ, Kim SH, Han MH.** Diffusion-weighted MRI in cystic or necrotic intracranial lesions. Neuroradiology 2000, **42**, 716-721.
11. **Schaefer PW, Grant PE, Gonzalez RG.** Diffusion-weighted MR imaging of the brain. Radiology 2000, **217**, 331-345.
12. **Sener RN.** Herpes simplex encephalitis: diffusion MR imaging findings. Comput Med Imaging Graph 2001, **25**, 391-397.
13. **Sutherland-Smith J, King R, Faissler D, Ruthazer R, Sato A.** Magnetic resonance imaging apparent diffusion coefficients for histologically confirmed intracranial lesions in dogs. Vet Radiol Ultrasound 2011, **52**, 142-148.
14. **Tsuchiya K, Katase S, Yoshino A, Hachiya J.** Diffusion-weighted MR imaging of encephalitis. AJR Am J Roentgenol 1999, **173**, 1097-1099.
15. **Wisner ER, Dickinson PJ, Higgins RJ.** Magnetic resonance imaging features of canine intracranial neoplasia. Vet Radiol Ultrasound 2011, **52** (Suppl 1), S52-61.